5th generation district heating and cooling network planning: A Dantzig-Wolfe decomposition approach

Marco Wirtz[a,b,*], Miguel Heleno[b], Alexandre Moreira[b], Thomas Schreiber[a], Dirk Müller[a]

[a] *RWTH Aachen University, E.ON Energy Research Center, Institute for Energy Efficient Buildings and Indoor Climate, Mathieustr. 10, Aachen, Germany*

[b] *Lawrence Berkeley National Laboratory, University of California, 1 Cyclotron Road, Berkeley, USA*

Abstract

The planning process of district energy systems with thermal networks is a challenging task. A proven method to include the dynamic behavior of energy systems in the planning process is mathematical optimization. However, especially for 5th generation district heating and cooling (5GDHC) networks, design optimization models become complex since they cover multiple building energy systems, a thermal and electrical network as well as central heating and cooling units. As a result, optimization models for large districts can become computationally intractable. To tackle this challenge and to reduce computational times, decomposition methods can be employed. In this paper, the Dantzig-Wolfe decomposition is used to transform a mixed-integer linear program into multiple subproblems (for every building) and a master problem (thermal and electrical network and central units). We consider a realistic case study based on a 5GDHC system in Germany. In this case study, we demonstrate that the proposed decomposition approach yields the same results attained by the original not decomposed problem. In addition, the scalability of the decomposition approach is investigated. It is found that the computational time of the decomposed formulation increases linearly for a number of buildings up to 100 and a number of design days up to 25. As a result, the decomposition approach leads to substantially smaller computational times for larger districts compared to the full model formulation. In general, the study results show the potential of the Dantzig-Wolfe decomposition to reduce computational times for design but also operational optimization models for 5GDHC networks.

*Corresponding author

Email address: marco.wirtz@eonerc.rwth-aachen.de (Marco Wirtz)

Keywords:
Dantzig-Wolfe decomposition, design optimization, MILP, 5GDHC, district heating, low-temperature heat network

1. Introduction

District heating and cooling (DHC) systems have a large potential to support the decarbonization of the heating and cooling sector which represents 50 % of the final energy consumption in Europe [1]. For urban as well as rural districts, DHC can reduce primary energy demands as well as local emissions [2]. In the development of district heating technologies, a trend towards lower network supply temperatures is observed [3]. Modern low-temperature networks make it possible to reduce heat losses and to integrate renewable low-temperature heat sources such as waste heat or geothermal energy [4, 5]. On the path towards lower network temperatures, the concept of 5th generation district heating and cooling (5GDHC) is receiving an increasing deal of attention in recent years [6, 7]. As discussed by Sulzer et al. [6], 5GDHC networks are known under various different terms, for example: *Bidirectional low-temperature network* ([8, 9, 10, 11]), *cold district heating* ([12], [13]), *anergy network* [14, 15, 16] *ambient loop*, *thermal microgrid*, or *termonet* [17]. The basic concept of 5GDHC networks is depicted in Fig. 1. The thermal network consists of a warm and a cold pipe with operating temperatures close to the ambient temperature of the ground (usually between -5 and 20 °C) which keeps heat losses to a minimum. Buildings with a heat demand take water from the warm pipe as heat source for the water-to-water heat pumps, that are installed in every building. Buildings with a cooling demand feed-in heat either with a chiller or a heat exchanger (direct cooling). The 5GDHC network therefore makes it possible to exchange heat between buildings and to reuse waste heat of buildings by other buildings in the district.

1.1. Design models for 5GDHC networks

The interconnection between buildings and the bidirectional energy flows poses challenges to district energy planners. Planning methods used for conventional district heating networks fall short since they do not account for time-dependent effects such as the balancing of heating and cooling demands between buildings. Therefore, recent publications focus

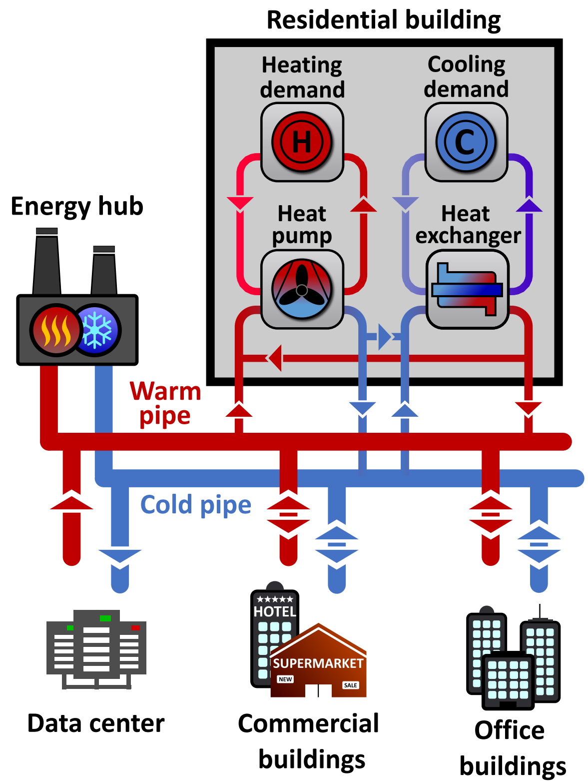

Figure 1: Principle of 5th generation district heating and cooling systems with heat and cold consumers and a central supply unit (energy hub). Illustration based on [18].

on developing new planning methods for districts with 5GDHC networks. Some papers use dynamic network simulations to support the planning process, while other models use mathematical optimization: Hering et al. [19] present a mixed-integer quadratically constrained program (MIQCP) to account not only for energy flows but also temperature constraints of a 5GDHC network. In their study, the buildings are aggregated in 3 building groups. The computational times vary strongly depending on the objective function and exceeds 1 hour in case of CO_2 emission minimization. Wirtz et al. [18] present a linear program for the design of a 5GDHC district considering all building energy systems (BESs) and the energy hub in a single model. For a case study with 17 buildings, the linear program comprises 530,000 decision variables and is solved in about 1 minute. In addition, mixed-integer linear programs (MILPs) and MIQCPs for operational optimization have been developed. However, even for small districts with only a few buildings, the models resulted in high computational times:

Gabrielli et al. [20] propose a MILP for the operational optimization of a 5GDHC network at ETH Zurich. For a district with 5 aggregated building blocks, they have to make substantial simplifications to obtain a model that is computationally tractable. Wirtz et al. [21] developed a MILP to optimize the annual network temperature profiles for a 5GDHC district with 17 buildings. For the optimization of a single control interval of 6 h, the computational time is about 5 minutes. Hering et al. [22] present another MIQCP which also aims at optimizing the network temperatures of a 5GDHC network. The computational times range between 350 and 10,000 s for a time horizon of one day. These studies show that the coupling of multiple BESs within districts with 5GDHC network leads to high computational times even for districts with a low number of buildings. High computational times are particularly problematic in the early phases of district planning, which typically require numerous design iterations. While model simplifications can drastically reduce the model complexity and solution times [23], they can only be used to a limited extent. Another proven approach to reduce computational complexity is to decompose (mixed-integer) linear programs into multiple smaller subproblems. The subproblems can then be solved separately from each other which also allows for parallelization of the calculation.

1.2. Dantzig-Wolfe decomposition for energy system models

A widely used approach to decompose large (mixed-integer) linear programs is the Dantzig-Wolfe decomposition [24]. In this approach, the block-angular structure of the constraint matrix is exploited to decompose the problem into multiple subproblems and a master problem that contains the coupling constraints. Dantzig-Wolfe decomposition has been used in a number of papers for energy system design: Yokoyama et al. [25] apply decomposition to a single-node energy supply system with a large number of technologies. For every component, a subproblem is formulated, which determines if the component is installed and its operation schedule. The master problem combines the subproblems of all components and provides coupling constraints such as energy balances. Harb et al. [26] solve an operational optimization problem of a district energy system by means of a Dantzig-Wolfe decomposition-based approach. They implement a solution algorithm based on Belov et al. [27] which enables to include integer variables in the problem formulation. In their study, they show that the computational time can be substantially reduced compared to the original (full) model formulation. However, the problem formulation does not consider installation or sizing decisions of the technologies. Schütz et al. [28] apply the Dantzig-Wolfe decomposition to a district energy system with a microgrid in which the BESs form the subproblems. The energy balances of the microgrid represent the master problem which optimizes the electricity exchange between buildings. While the authors only consider electricity exchange between buildings, they propose to apply the method also to local heating networks in the future. The following two recently published papers address design problems that include heat exchange between decentral energy supply systems: Wakui et al. [29] decompose a large-scale design problem using Dantzig-Wolfe decomposition. The master problem determines the power and heat exchange between different energy supply systems and the subproblems optimize the energy supply system design. In addition, Dantzig-Wolfe decomposition was applied to stochastic design problems in which the uncertainty scenarios are represented by subproblems. In another paper, Wakui et al. [30] use a similar approach and show that the decomposition approach leads to lower operational costs compared to the equivalent full formulation since the decomposed formulation converges faster.

Decomposition techniques can play an instrumental role in alleviating the challenges associated with model scalability and computational tractability that are usually faced in studies that address 5GDHC systems. However, to the best of our knowledge, decomposition approaches to design 5GDHC networks have not been proposed yet. As a consequence, models that deal with these systems either have to constrain their application to small-scale system with limited usefulness [21, 22, 20, 19] or rely on substantial model simplifications [18]. Thus, decomposition approaches have the potential to unlock model development to address problems related to 5GDHC networks. Hence, in this paper we propose a Dantzig-Wolfe decomposition-based approach to design 5GDHC networks as an alternative to avoid directly solving a large scale MILP. The contributions of this study are presented in the following section.

1.3. Contributions

The contributions of this study are summarized as follows:

- A Dantzig-Wolfe decomposition-based efficient approach to design district systems with 5GDHC network. The resulting optimization models of the master and subproblems are described in detail and validated with the corresponding full model formulation.

- A sensitivity analysis is conducted to investigate how the solution times of the Dantzig-Wolfe decomposition vary with the number of buildings and the temporal resolution of the model (number of design days).

- Shadow prices for heat, cold (in case of negative heat prices) and electricity, which result from the master problem, are analyzed within a case study. The shadow prices can be interpreted as market clearing prices for heat and electricity in the district. Since pricing models are not trivial for 5GDHC districts with prosumer buildings, the analysis of shadow prices as a byproduct of the optimization model can help decision makers to design appropriate pricing models.

1.4. Paper organization

The paper is structured as follows: In Section 2, the full model formulation as well as the decomposed master and subproblems are presented in detail. The decomposition approach is applied to a case study which is introduced in Section 3. The results of the case study as well as a sensitivity analysis are presented and discussed in Section 4. Finally, Section 5 provides conclusions and an outlook on future works.

2. Methods

In this section, the full model formulation as well as the decomposed models are presented. In both cases, the optimization model determines the optimal energy system configuration in the connected buildings as well as the energy hub to cover time-varying heating and cooling demands of the buildings. The optimal system configuration is described by the investment decision resulting from which technologies are installed and how they are dimensioned. For this study, in all models a time resolution of $\Delta t = 1$ hour is used.

The model uses technology superstructures from which the optimal technologies are selected. In the following description of the objective function and the model constraints, all decision variables of the model are constrained to have non-negative values unless otherwise stated. In Section 2.1, the full formulation is introduced and in Section 2.2, the proposed Dantzig-Wolfe decomposition-based approach is described.

2.1. Full model formulation

The full formulation is a MILP that includes the design problem of the energy hub and the BESs in a single model. In the following, the objective function is introduced first and thereafter, the model constraints are described in detail.

2.1.1. Objective function

The objective function of the full model formulation represents total annualized costs C_{tot} using the definition by the German standard VDI 2067 [31]. The total annualized costs comprise costs for the equipment of the energy hub and of the BESs (C_{EH}, C_{BES}) as well as costs for electricity import from the national grid (C_{el}). Revenues result from electricity feed-in ($R_{\text{feed-in}}$):

$$\min C_{\text{tot}} = C_{\text{EH}} + C_{\text{BES}} + C_{\text{el}} - R_{\text{feed-in}} \tag{1}$$

The annualized equipment costs include annualized investment costs as well as operation and maintenance costs:

$$C_{\text{EH}} = \sum_{k \in K_{\text{EH}}} \left(C_{\text{inv},k} + C_{\text{om},k}\right) \tag{2}$$

$$= \sum_{k \in K_{\text{EH}}} \left(c_{\text{inv},k,\text{EH}}\; cap_{k,\text{EH}}\right)\left(a_{\text{inv},k} + f_{\text{om},k}\right) \tag{3}$$

Here, the set $K_{\text{EH}} = \{\text{ASHP, PV, ACC, BAT}\}$ contains all energy hub technologies and cap_k denotes the nominal capacity of each technology k: For the air-source heat pump and photovoltaic modules, cap_k refers to the rated electric power ($P^{\text{nom}}_{\text{ASHP,EH}}$, $P^{\text{nom}}_{\text{PV,EH}}$), and for energy storages (ACC, BAT), cap_k is the storage capacity ($S^{\text{cap}}_{\text{ACC,EH}}$, $S^{\text{cap}}_{\text{BAT,EH}}$). For all technologies, constant specific investment costs are used $c_{\text{inv},k}$.

The factor $a_{\text{inv},k}$ denotes the annuity factor and $f_{\text{om},k}$ the annual cost share for maintenance costs. Similarly, the costs of the BESs are:

$$C_{\text{BES}} = \sum_{b \in \mathcal{B}} \sum_{k \in K_{\text{BES}}} \left(c_{\text{inv},k,\text{BES}}\; cap_{k,b} + x_{k,b}\; c^{\text{fix}}_{\text{inv},k,\text{BES}}\right)\left(a_{\text{inv},k} + f_{\text{om},k}\right) \tag{4}$$

Here, $x_{k,b}$ is a binary variable that indicates if the technology is installed ($x_{k,b} = 1$) or not ($x_{k,b} = 0$) and $c^{\text{fix}}_{\text{inv},k,\text{BES}}$ describes fix investment costs. The set K_{BES} comprises all technologies of the BESs, i. e. heat pump, heat storage and electric heater.

The cost for electricity import from the main grid results from the import power $P_{\text{grid},d,t}$ and a time-varying electricity price ($p_{\text{el},d,t}$).

$$C_{\text{el}} = \sum_{d\in\mathcal{D}} w_d \sum_{t\in\mathcal{T}} P_{\text{grid},d,t}\ p_{\text{el},d,t} \Delta t \tag{5}$$

Here, w_d denotes the number of days represented by the design day d. Revenues from electricity sales result from the feed-in power $P_{\text{feed-in},d,t}$ and the feed-in tariff $r^{\text{feed-in}}_{\text{el},d,t}$:

$$R_{\text{feed-in}} = \sum_{d\in\mathcal{D}} w_d \sum_{t\in\mathcal{T}} P_{\text{feed-in},d,t}\ r^{\text{feed-in}}_{\text{el},d,t} \Delta t \tag{6}$$

2.1.2. Model constraints

The model comprises constraints for the BESs, the energy hub as well as the 5GDHC network and electrical microgrid.

Building energy system

In the BESs, heat pumps, electric heaters and thermal energy storages provide heat. The heat pump is connected to the 5GDHC network and increases the temperature of the heat from the network. The electric heater can cover peak demands and may use low electricity prices to charge the heat storage. Cooling is provided by a heat exchanger (direct cooling, DRC) that is thermally connected with the cold pipe of the 5GDHC network. The resulting superstructure is depicted in Fig. 2.

If a technology is built, the binary installation variable $x_{k,b}$ is forced to 1 using a big-M constraint with $\hat{\text{M}}$ sufficiently large:

$$cap_{k,b} \leq x_{k,b}\ \hat{\text{M}} \quad \forall\ b \in \mathcal{B},\ \ k \in K_{\text{BES}} \tag{7}$$

The electricity consumption ($P_{k,b,d,t}$) of the heat pump and electric boiler is bound by their nominal power ($P^{\text{nom}}_{k,b}$):

$$P_{\text{HP},b,d,t} \leq P^{\text{nom}}_{\text{HP},b} \quad \forall\ b \in \mathcal{B},\ \ d \in \mathcal{D},\ \ t \in \mathcal{T} \tag{8}$$

$$P_{\text{EB},b,d,t} \leq P^{\text{nom}}_{\text{EB},b} \quad \forall\ b \in \mathcal{B},\ \ d \in \mathcal{D},\ \ t \in \mathcal{T} \tag{9}$$

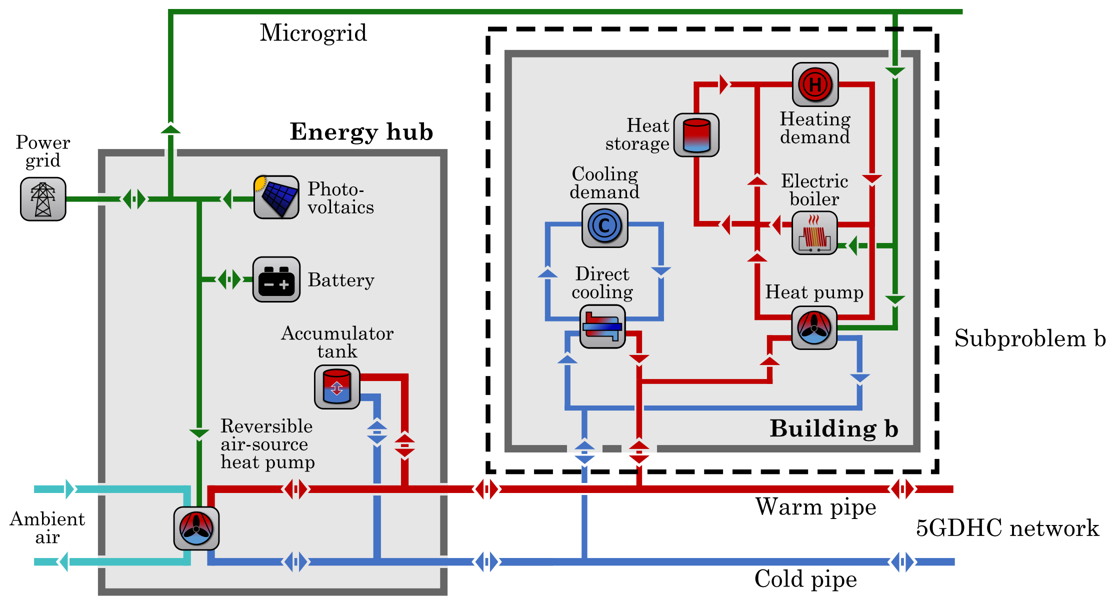

Figure 2: Superstructure of the design problem with all technologies of the energy hub and BESs. The 5GDHC network provides heating and cooling energy for the buildings, the microgrid connects all buildings with the energy hub. In the decomposition approach, every building forms a subproblem.

Assuming a constant thermal efficiency for electric heaters and a temperature-dependent coefficient of performance (COP) for the heat pumps, the heat generation $\dot{Q}_{\mathrm{h},k,b,d,t}$ is:

$$\dot{Q}_{\mathrm{h,HP},b,d,t} = P_{\mathrm{HP},b,d,t}\; COP_{\mathrm{HP},b,d,t} \quad \forall\; b \in \mathcal{B},\;\; d \in \mathcal{D},\;\; t \in \mathcal{T} \tag{10}$$

$$\dot{Q}_{\mathrm{h,EB},b,d,t} = P_{\mathrm{EB},b,d,t}\; \eta_{\mathrm{EB}} \quad \forall\; b \in \mathcal{B},\;\; d \in \mathcal{D},\;\; t \in \mathcal{T} \tag{11}$$

Minimum part-load constraints ensure that the heat pump's operation is bound to a reasonable operation range. For this purpose, the binary variables $u_{\mathrm{HP},b,d,t}$ are introduced to indicate if the heat pump is operated at a given time step t ($u_{\mathrm{HP},b,d,t} = 1$) or not ($u_{\mathrm{HP},b,d,t} = 0$). If it is operated, the electric demand must be larger than the minimum part-load threshold $\mathrm{PLR_{HP}}$. This results in the following disjunctive constraints with $\hat{\mathrm{M}}$ being a sufficiently large number:

$$\mathrm{PLR_{HP}} P^{\mathrm{nom}}_{\mathrm{HP},b} \leq P_{\mathrm{HP},b,d,t} + \hat{\mathrm{M}}(1 - u_{\mathrm{HP},b,d,t}) \quad \forall\; b \in \mathcal{B},\;\; d \in \mathcal{D},\;\; t \in \mathcal{T} \tag{12}$$

$$P_{\mathrm{HP},b,d,t} \leq u_{\mathrm{HP},b,d,t}\hat{\mathrm{M}} \quad \forall\; b \in \mathcal{B},\;\; d \in \mathcal{D},\;\; t \in \mathcal{T} \tag{13}$$

Heat storages are modeled as ideally stratified and the storage capacity is denoted by

$S^{\mathrm{cap}}_{\mathrm{TES},b}$. The state of charge $S_{\mathrm{TES},b,d,t}$ is bound by the nominal storage capacity which yields:

$$S_{\mathrm{TES},b,d,t} \leq S^{\mathrm{cap}}_{\mathrm{TES},b} \quad \forall\, b \in \mathcal{B},\ d \in \mathcal{D},\ t \in \mathcal{T} \tag{14}$$

The energy balance for the heat storage for time steps $t > 1$ is:

$$\begin{aligned} S_{\mathrm{TES},b,d,t} = {} & S_{\mathrm{TES},b,d,t-1}(1 - \phi_{\mathrm{TES,loss}}) \\ & + \eta^{\mathrm{ch}}_{\mathrm{TES}} \dot{Q}^{\mathrm{ch}}_{\mathrm{h,TES},b,d,t} - \frac{\dot{Q}^{\mathrm{dch}}_{\mathrm{h,TES},b,d,t}}{\eta^{\mathrm{dch}}_{\mathrm{TES}}} \\ & \forall\, b \in \mathcal{B},\ d \in \mathcal{D},\ t \in \mathcal{T} \end{aligned} \tag{15}$$

Here, the charging and discharging heat flows are denoted by $\dot{Q}^{\mathrm{ch}}_{\mathrm{h,TES},b}$ and $\dot{Q}^{\mathrm{dch}}_{\mathrm{h,TES},b}$, respectively. $\eta^{\mathrm{ch}}_{\mathrm{TES}}$ and $\eta^{\mathrm{dch}}_{\mathrm{TES}}$ are charging and discharging efficiencies; $\phi_{\mathrm{TES,loss}}$ are stand-by heat losses. Furthermore, it is assumed that the state of charge at the beginning of each design day is equal to the state of charge at the end of the day (cyclic condition). The state of charge at the beginning of the design day is the same for all design days and is a decision variable in the model. The heat balances for the buildings ensure that all demands $\dot{Q}_{\mathrm{h,dem},b,d,t}$ are met:

$$\begin{aligned} & \dot{Q}_{\mathrm{h,HP},b,d,t} + \dot{Q}_{\mathrm{h,EB},b,d,t} + \dot{Q}^{\mathrm{dch}}_{\mathrm{h,TES},b,d,t} = \\ & \dot{Q}_{\mathrm{h,dem},b,d,t} + \dot{Q}^{\mathrm{ch}}_{\mathrm{h,TES},b,d,t} \quad \forall\, b \in \mathcal{B},\ d \in \mathcal{D},\ t \in \mathcal{T} \end{aligned} \tag{16}$$

For cooling, it is assumed that all demands $\dot{Q}_{\mathrm{c,dem},b,d,t}$ are met by the heat exchanger (direct cooling):

$$\dot{Q}_{\mathrm{c,dem},b,d,t} = \dot{Q}_{\mathrm{c,DRC},b,d,t} \quad \forall\, b \in \mathcal{B},\ d \in \mathcal{D},\ t \in \mathcal{T} \tag{17}$$

The net thermal demand of the buildings are covered by the 5GDHC network:

$$\begin{aligned} \dot{Q}_{\mathrm{res,BES},b,d,t} = {} & \dot{Q}_{\mathrm{h,HP},b,d,t} \left(1 - \frac{1}{COP_{\mathrm{HP},b,d,t}}\right) \\ & - \dot{Q}_{\mathrm{c,DRC},b,d,t} \quad \forall\, b \in \mathcal{B},\ d \in \mathcal{D},\ t \in \mathcal{T} \end{aligned} \tag{18}$$

Here, the residual thermal building demand ($\dot{Q}_{\mathrm{res,BES},b,d,t}$) is a free variable and can take positive or negative values. The electricity demand of the building is

$$P_{\mathrm{BES},b,d,t} = P_{\mathrm{EB},b,d,t} + P_{\mathrm{HP},b,d,t} \quad \forall\, b \in \mathcal{B},\ d \in \mathcal{D},\ t \in \mathcal{T} \tag{19}$$

and is covered by the electric microgrid.

Thermal network and microgrid

The energy hub supplies the residual thermal demands of all buildings, which are not balanced within the network, plus thermal losses of the network itself:

$$\dot{Q}_{\mathrm{res,EH},d,t} = \sum_{b \in \mathcal{B}} \dot{Q}_{\mathrm{res,BES},b,d,t} + \dot{Q}_{\mathrm{h,loss},d,t} - \dot{Q}_{\mathrm{c,loss},d,t} \quad \forall\, d \in \mathcal{D},\ t \in \mathcal{T} \tag{20}$$

The microgrid is modelled by a single energy balance aggregating the electricity demands of all buildings:

$$P_{\mathrm{res,EH},d,t} = \sum_{b \in \mathcal{B}} P_{\mathrm{BES},b,d,t} \quad \forall\, d \in \mathcal{D},\ t \in \mathcal{T} \tag{21}$$

Energy hub

The superstructure of the energy hub includes a reversible heat pump for generating heat and cold, a thermal storage, as well as photovoltaics (PV) and a battery. The superstructure is illustrated in Fig. 2. In addition, electricity can be imported from or fed into the national electricity grid.

The electricity demand of the air-source heat pump as well as the power generation by PV modules is limited by their rated electric power:

$$P_{\mathrm{ASHP,EH},d,t} \leq P^{\mathrm{nom}}_{\mathrm{ASHP,EH}} \quad \forall\, d \in \mathcal{D},\ t \in \mathcal{T} \tag{22}$$

$$P_{\mathrm{PV,EH},d,t} \leq P^{\mathrm{nom}}_{\mathrm{PV,EH}} \quad \forall\, d \in \mathcal{D},\ t \in \mathcal{T} \tag{23}$$

The heating ($\dot{Q}_{\mathrm{h,ASHP,EH},d,t}$) and cooling power ($\dot{Q}_{\mathrm{c,ASHP,EH},d,t}$) of the air-source heat pump is given by:

$$\dot{Q}_{\mathrm{h,ASHP,EH},d,t} = P_{\mathrm{h,ASHP,EH},d,t}\, COP_{\mathrm{h,ASHP},d,t} \quad \forall\, d \in \mathcal{D},\ t \in \mathcal{T} \tag{24}$$

$$\dot{Q}_{\mathrm{c,ASHP,EH},d,t} = P_{\mathrm{c,ASHP,EH},d,t}\, COP_{\mathrm{c,ASHP},d,t} \quad \forall\, d \in \mathcal{D},\ t \in \mathcal{T} \tag{25}$$

The electricity demand of the air-source heat pump is:

$$P_{\mathrm{ASHP,EH},d,t} = P_{\mathrm{h,ASHP,EH},d,t} + P_{\mathrm{c,ASHP,EH},d,t} \quad \forall\, d \in \mathcal{D},\ t \in \mathcal{T} \tag{26}$$

The power of the PV modules ($P_{\mathrm{PV,EH},d,t}$) is constrained by the specific generation power per kW$_\mathrm{p}$ ($p_{\mathrm{PV,gen},d,t}$) multiplied by the capacity of the PV modules:

$$P_{\mathrm{PV,EH},d,t} \leq p_{\mathrm{PV,gen},d,t} P^{\mathrm{nom}}_{\mathrm{PV,EH}} \quad \forall\ d \in \mathcal{D},\ \ t \in \mathcal{T} \tag{27}$$

The generation profile of PV is calculated prior to the optimization. The PV capacity is limited by an upper bound which results from the available space for PV installations:

$$P^{\mathrm{nom}}_{\mathrm{PV,EH}} \leq P^{\mathrm{nom,max}}_{\mathrm{PV,EH}} \tag{28}$$

The energy storages in the energy hub are modeled using an approach by Gabrielli et al. [32] that allows to consider seasonal operation despite using design days. For this purpose, the function $\sigma : Y \rightarrow \mathcal{D}$, $\sigma(y) = d$ is introduced which maps 365 days to their respective design day based on the k-medoids design day clustering. Here, the set $Y = \{1, 2, ..., 365\}$ represents all days of the year. The state of charge of the storages at time step t results from the state of charge of the previous time step $(t-1)$:

$$\begin{aligned} S_{k,\mathrm{EH,y,t}} = {} & S_{k,\mathrm{EH,y,t-1}} \left(1 - \phi_{k,\mathrm{EH,loss}}\right) \\ & + \eta^{\mathrm{ch}}_{k,\mathrm{EH}} P^{\mathrm{ch}}_{k,\mathrm{EH},\sigma(y),t} - \frac{P^{\mathrm{dch}}_{k,\mathrm{EH},\sigma(y),t}}{\eta^{\mathrm{dch}}_{k,\mathrm{EH}}} \\ & \forall\ \ k \in \{\mathrm{ACC, BAT}\}, \quad y \in \mathrm{Y}, \quad t \in \mathcal{T} \setminus \{1\} \end{aligned} \tag{29}$$

Here, $P^{\mathrm{ch}}/P^{\mathrm{dch}}$ denotes charging and discharging flows of the respective storage. For the heat storage, these are $\dot{Q}^{\mathrm{ch}}_{\mathrm{h,ACC,EH}}/\dot{Q}^{\mathrm{dch}}_{\mathrm{h,ACC,EH}}$ and for the battery $P^{\mathrm{dch}}_{\mathrm{BAT,EH}}/P^{\mathrm{ch}}_{\mathrm{BAT,EH}}$. The transition between the first time step of day y and the last time step of the previous day $(y-1)$ is modeled by:

$$\begin{aligned} S_{k,\mathrm{EH,y,1}} = {} & S_{k,\mathrm{EH,y-1,24}} \left(1 - \phi_{k,\mathrm{EH,loss}}\right) \\ & + \eta^{\mathrm{ch}}_{k,\mathrm{EH}} P^{\mathrm{ch}}_{k,\mathrm{EH},\sigma(y),1} - \frac{P^{\mathrm{dch}}_{k,\mathrm{EH},\sigma(y),1}}{\eta^{\mathrm{dch}}_{k,\mathrm{EH}}} \\ & \forall\ \ k \in \{\mathrm{ACC, BAT}\}, \quad y \in \mathrm{Y} \setminus \{1\} \end{aligned} \tag{30}$$

Finally, the cyclic condition ensures the connection between the first time step of the first day of the year with the last time step of the 365th day:

$$\begin{aligned} S_{k,\mathrm{EH},1,1} = {} & S_{k,\mathrm{EH},365,24} \left(1 - \phi_{k,\mathrm{EH,loss}}\right) \\ & + \eta^{\mathrm{ch}}_{k,\mathrm{EH}} P^{\mathrm{ch}}_{k,\mathrm{EH},\sigma(1),1} - \frac{P^{\mathrm{dch}}_{k,\mathrm{EH},\sigma(1),1}}{\eta^{\mathrm{dch}}_{k,\mathrm{EH}}} \\ & \forall \;\; k \in \{\mathrm{ACC}, \mathrm{BAT}\} \end{aligned} \tag{31}$$

In case of the battery, the storage capacity is limited by a lower bound:

$$S^{\mathrm{cap,min}}_{\mathrm{BAT,EH}} \leq S^{\mathrm{cap}}_{\mathrm{BAT,EH}} \tag{32}$$

Energy balances

A thermal energy balance ensures that all heating and cooling demands of the 5GDHC network are covered:

$$\begin{aligned} & \dot{Q}_{\mathrm{h,ASHP,EH},d,t} + \dot{Q}^{\mathrm{dch}}_{\mathrm{h,TES,EH},d,t} = \\ & \dot{Q}_{\mathrm{res,EH},d,t} - \dot{Q}_{\mathrm{c,ASHP,EH},d,t} + \dot{Q}^{\mathrm{ch}}_{\mathrm{h,TES,EH},d,t} \quad \forall \; d \in \mathcal{D}, \;\; t \in \mathcal{T} \end{aligned} \tag{33}$$

As introduced in the thermal network constraints, $\dot{Q}_{\mathrm{res,EH},d,t}$ describes the heating (positive value) or cooling (negative value) load of the 5GDHC network. The electricity demands of the microgrid as well as the air-source heat pump in the energy hub are covered by PV or electricity imports from the national grid ($P_{\mathrm{grid},d,t}$):

$$\begin{aligned} & P_{\mathrm{PV,EH},d,t} + P_{\mathrm{grid},d,t} + P^{\mathrm{dch}}_{\mathrm{BAT,EH},d,t} = \\ & P_{\mathrm{res,EH},d,t} + P_{\mathrm{feed-in},d,t} + P^{\mathrm{ch}}_{\mathrm{BAT,EH},d,t} \quad \forall \; d \in \mathcal{D}, \;\; t \in \mathcal{T} \end{aligned} \tag{34}$$

Here, $P^{\mathrm{ch}}_{\mathrm{BAT,EH},d,t}/P^{\mathrm{dch}}_{\mathrm{BAT,EH},d,t}$ and denote the charging and discharging power of the battery, respectively.

2.2. Dantzig-Wolfe reformulation and Column Generation

In the following sections, the Dantzig-Wolfe reformulation is introduced (Section 2.2.1) and the resulting master and subproblems are presented in Sections 2.2.2 and 2.2.3, respectively.

2.2.1. Derivation of master and subproblem

The full formulation of the problem described in Section 2.1 can be written in a compact form as follows:

$$\min c^T x \tag{35}$$

$$\text{s.t.} \quad \begin{pmatrix} B_1 & B_2 & \cdots & B_n \\ A_1 & & & \\ & A_2 & & \\ & & \ddots & \\ & & & A_n \end{pmatrix} \begin{pmatrix} x_0 \\ x_1 \\ x_2 \\ \vdots \\ x_n \end{pmatrix} = \begin{pmatrix} b_0 \\ b_1 \\ b_2 \\ \vdots \\ b_n \end{pmatrix} \tag{36}$$

where A is the coefficient matrix, x the vector of decision variables, and b the right-hand-side vector. The coefficient matrix of the full formulation has a block-angular structure: The design problem of a BES forms almost an isolated problem. The building constraints are only coupled with the rest of the problem by the decision variables that describe the energy imports from the electric and thermal grid. A method to solve large-scale optimization problems with a block-angular structure is the Dantzig-Wolfe decomposition. In this method, instead of solving the problem in a single solution process, the problem is split into a master problem and multiple subproblems. The subproblems represent the blocks on the matrix diagonal A_i and the master problem consists of the coupling constraints

$$B_1 x_1 + B_1 x_2 + ... + B_n x_n = b_0. \tag{37}$$

The main idea of the decomposition method is to generate multiple solutions for the subproblems and to recombine them in order to get an optimal solution for the entire problem. The Dantzig-Wolfe decomposition is based on a theorem by Minkwoski which states that every compact convex set is the convex hull of its set of extreme points [33]. For the optimization problem, this means that all solutions x of the feasible solution space can be described by a convex combination of the extreme points x_j of the full formulation which can be written as:

$$x_i = \sum_j \lambda_j x_j \tag{38}$$

$$\sum_j \lambda_j = 1 \tag{39}$$

$$\lambda_j \geq 0 \tag{40}$$

Applying the Minkowski theorem to the original problem in Eq. (36), we obtain the master problem:

$$\min \quad \sum_{i=1}^{n} \sum_{j=1}^{p_i} \lambda_{i,j} (c_i^T x_{i,j}) \tag{41}$$

$$\sum_{j=1}^{p_i} \lambda_{i,j} = 1 \quad \forall\, i \in \{1, 2, ..., n\} \tag{42}$$

$$\lambda_{i,j} \geq 0 \quad \forall\, i, j \tag{43}$$

This leads to a problem with a large number of variables, i. e. extreme points $\lambda_{i,j}$. However, the obtained formulation can be solved using a column generation approach. This means that not all extreme points (columns) have to be calculated to solve the problem but that extreme points are generated iteratively as they lead to reduced costs in the objective function of the master problem. From the dual formulation of the master problem, the reduced costs are then:

$$\begin{pmatrix} c_1^T x_{1,j} - \pi_1 \sigma^T B_1 x_{1,j} \\ c_2^T x_{2,j} - \pi_2 \sigma^T B_2 x_{2,j} \\ \vdots \\ c_n^T x_{n,j} - \pi_n \sigma^T B_n x_{n,j} \end{pmatrix} \tag{44}$$

First, the full master problem is solved for a limited amount of extreme points. With a solution of this reduced master problem, the dual variables are determined and new columns can be generated by solving the subproblems and finding an optimal solution for:

$$\min \quad c_i^T x_i - \pi_i - \sigma^T B_i x_i \tag{45}$$

$$A_i x_i = b_i \tag{46}$$

$$x_i \geq 0 \tag{47}$$

The subproblems can be solved with low computational effort and the solution process of multiple suproblems can be parallelized. Every subproblem proposes another column, which - if it leads to negative reduced costs - is added to the master problem. The algorithm terminates when the subproblems do not provide any new columns, or alternatively when a certain convergence criterion is met, such as a maximum number of iterations or a marginal improvement of the objective function of the master problem. In this study, a maximum number of iterations as well as a threshold for further improvement in the objective function of the master problem is used. The solution process of the column generation approach is depicted in Fig. 3 and is based on studies by Harb et al. [34] and Schütz et al. [28]: In a first step, the master problem is initialized and solved. The shadow prices are obtained from the solution of the master problem. Shadow prices are the constraint dual values of a solution and are therefore also called *dual price*. With the shadow prices, the subproblems are set up. The solution of the subproblems are returned to the master problem and the master problem is solved again. In the master problem, the solutions of the subproblems are weighted with the continuous weights $\lambda_{i,j}$. Since the subproblems are mixed-integer linear programs, feasibility of the master problem is not ensured for continuous weights. Therefore, in a final step, the master problem is solved with binary weights ($\lambda_{i,j} \in \{0, 1\}$). Theoretically, optimality is not guaranteed when the weights are binary and the subproblems contain binary variables as well. However, previous studies indicated that this solution process leads to near-optimal solutions [34, 28]. Applied to a district with 5GDHC network and microgrid, the proposed decomposition approach provides shadow prices for each time step. These shadow prices generated by the master problem steer the solution of the subproblems and can be interpreted as the price for heat and electricity for the buildings. In addition, the prices of the converged solution can then be interpreted as market clearing prices for heat and electricity.

2.2.2. Master problem

The objective function of the master problem includes investment and maintenance cost for the technologies of the energy hub (C_{EH}) and BESs ($C_{\mathrm{BES,tot}}$) as well as electricity costs

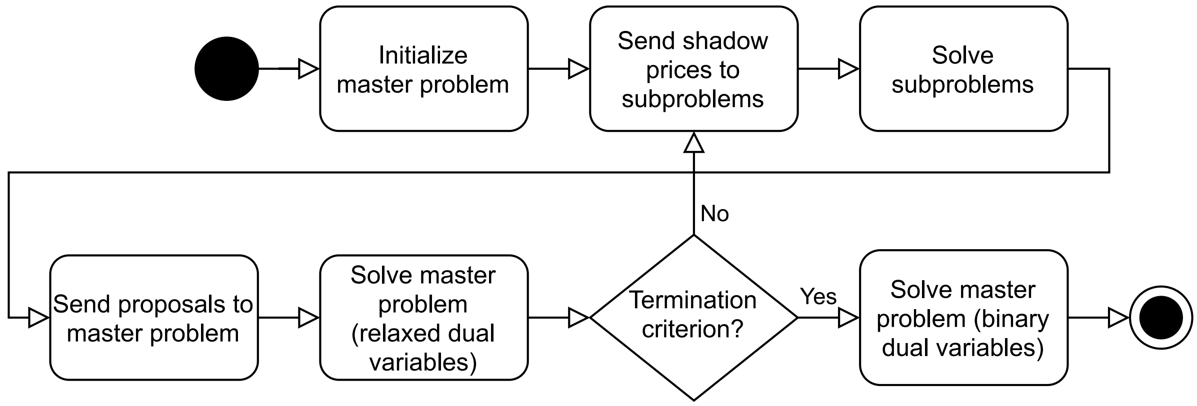

Figure 3: Algorithm of the iterative column generation process.

(C_{el}) and revenues from electricity feed-in $R_{\text{feed-in}}$:

$$\min C_{\text{tot}} = C_{\text{EH}} + C_{\text{BES,tot}} + C_{\text{el}} - R_{\text{feed-in}} \tag{48}$$

The constraints for the investment and maintenance costs in the energy hub as well as the electricity cost and revenues for electricity import and feed-in are adopted from the full model formulation, i. e. Eqs. (2), (5) and (6). The investment and maintenance costs of the building technologies are summed over all buildings and all weighted proposals:

$$C_{\text{BES,tot}} = \sum_{b \in \mathcal{B}} \sum_{p \in \mathcal{P}} C_{\text{BES},b,p}\, \lambda_{p,b} \tag{49}$$

For the continuous weights, the convexity constraints are added:

$$\lambda_{p,b} \leq 1 \quad \forall\, p \in \mathcal{P},\;\; b \in \mathcal{B} \tag{50}$$

$$\sum_{p \in \mathcal{P}} \lambda_{p,b} = 1 \quad \forall\, b \in \mathcal{B} \tag{51}$$

In addition, the technology constraints (22) – (28) as well as the storage constraints (29) – (32) of the full formulation are included in the master problem. The master problem also includes the thermal and electricity balance of the energy hub, i. e. constraints (33) and (34). However, constraints (20) and (21) of the full formulation are replaced by the corresponding constraints with the weighting factors:

$$\dot{Q}_{\text{res,EH},d,t} = \sum_{b \in \mathcal{B}} \sum_{p \in \mathcal{P}} \lambda_{p,b} \dot{Q}_{\text{res,BES},p,b,d,t} + \dot{Q}_{\text{h,loss},d,t} - \dot{Q}_{\text{c,loss},d,t}$$

$$\forall\, d \in \mathcal{D},\;\; t \in \mathcal{T} \tag{52}$$

$$P_{\text{res,EH},d,t} = \sum_{b\in\mathcal{B}} \sum_{p\in\mathcal{P}} \lambda_{p,b} P_{\text{BES},p,b,d,t} \quad \forall\, d \in \mathcal{D},\;\; t \in \mathcal{T} \tag{53}$$

2.2.3. Subproblems

Each solution of a subproblem represents a proposal p which is added to all subsequent master problems. Proposals comprise the cost of the building technologies (C_{BES}) as well as energy import profiles for heat and electricity ($\dot{Q}_{\text{res,BES},d,t}$ and $P_{\text{BES},d,t}$). The objective function of the subproblem is:

$$\min\left(C_{\text{tac}} - \sigma\right) \tag{54}$$

Here, σ is the shadow price derived from Eq. (51) of the previous master problem solution. The value of σ is individual for each building (subproblem). The total annual costs of the subproblem consist of the annualized investment and maintenance costs of the technologies (C_{BES}) as well as costs for heat and electricity imports (C_{heat}, C_{el}):

$$C_{\text{tac}} = C_{\text{BES}} + C_{\text{heat}} + C_{\text{el}} \tag{55}$$

The electricity costs in the subproblems are expressed with the shadow price for electricity $\pi_{\text{el},d,t}$ obtained from Eq. (53) of the previous master problem:

$$C_{\text{el}} = \sum_{d\in\mathcal{D}} w_d \sum_{t\in\mathcal{T}} P_{\text{BES},d,t} \pi_{\text{el},d,t} \Delta t \tag{56}$$

Likewise, the cost for heat import from the 5GDHC network is:

$$C_{\text{heat}} = \sum_{d\in\mathcal{D}} w_d \sum_{t\in\mathcal{T}} \dot{Q}_{\text{res,BES},d,t}\, \pi_{\text{heat},d,t}\, \Delta t \tag{57}$$

Here, $\pi_{\text{heat},d,t}$ denotes the shadow price for heat imports which is derived from Eq. (52) of the previous master problem. All additional building constraints of the full formulation (7) – (19), which are not connected to the coupling constraints or objective function, are added to each subproblem as well.

2.2.4. Limitations

Due to the low temperatures in 5GDHC networks, heat losses of the network are not dominant. This means, that the used formulation with static thermal losses and a single thermal energy balance is a valid approach in this model. However, for conventional district heating systems where heat losses have a crucial influence on the performance of the network, it might be necessary to consider heat losses for every individual pipe section. This will make the decomposition formulation more complex. As a result, the decomposition approach presented in this paper cannot be adapted to conventional district heating systems without modifications.

Moreover, the optimization approach does not differentiate between the network operator and the building owner. Instead, the model minimizes the total annualized costs of the heating and cooling supply in the district in general. Although this is a valid assumption for contracting solutions and is also widely used for design optimization models, the objective function and thus the optimal solution are affected by the differentiation of which stakeholder pays for which expenditures.

3. Case study

In this case study, we illustrate our proposed methodology to design a 5GDHC network located in the district *Shamrock Park* in the city of Herne, Germany. The district includes newly built and existing buildings. In total, 25 buildings will be connected to the 5GDHC network as depicted in Fig. 4. The building stock will comprise 10 offices, 10 residential buildings, 2 data centers, 2 hotels and 1 nursing home. For this study, slight simplifications to the case study have been made regarding the considered generation and storage technologies in the buildings and the energy hub in order to keep the model complexity low and facilitate the interpretation of the results, with respect to the decomposition method. Therefore in this study, the energy hub only comprises a reversible air-source heat pump to generate heat and cold, a thermal storage (accumulator tank), PV modules and a battery. The maximum photovoltaic capacity is assumed 2 $\mathrm{MW_p}$ and, due to resiliency considerations, the minimum battery capacity in the energy hub is 1 MWh. The operating temperatures of the 5GDHC networks are assumed constant throughout the year at 22 °C (warm pipe) and 12 °C (cold pipe). The temperatures affect the COP of the building heat pumps and the reversible air-source heat pump in the energy hub. The (heating) COP of the heat pump in the energy hub is calculated using the Carnot efficiency with an exergy efficiency of 0.4. The investment costs, technology life times and operation and maintenance costs of the energy conversion technologies are depicted in Table 1.

Table 1: Economic parameters of energy conversion technologies.

	ASHP	PV	HP (bldgs)	EB (bldgs)
Specific investment $\left(\frac{\text{EUR}}{\text{kW}}\right)$	350	750	350	25
Lifetime (a)	20	20	20	20
Maintenance (% of inv.)	2.5	1.0	2.5	1.0

The generation profiles for PV modules have been simulated prior to the optimization. For the thermal network, losses are calculated according to DIN EN 13941 [35]. The electricity price has a time resolution of one hour and is based on EEX spot price data. For the feed-in tariff, the electricity price is offset by an assumed market spread of 2 EUR-ct/kWh. For clustering design days, a k-medoids algorithm is employed as presented by Domínguez et al. [36] and implemented by Schütz et al. [37].

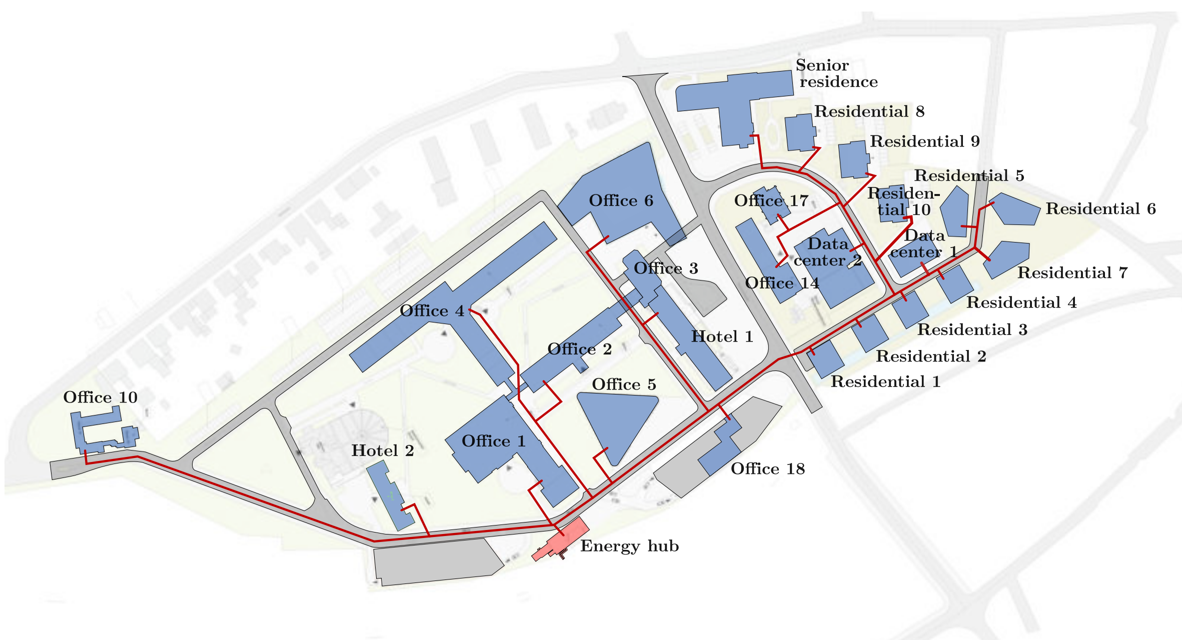

Figure 4: The district Shamrock Park in Herne (Germany) comprises 25 buildings and an energy hub.

The heating and cooling demand profiles were simulated using Modelica models created with TEASER [38] and the domestic hot water demand was simulated using DHWcalc [39].

The total annual space heating demand is 5.6 GWh (peak demand: 2.8 MW) and the total annual cooling demand 3.6 GWh (peak demand: 2.9 MW). The domestic hot water demand is 0.5 GWh per year. Fig. 5 shows the cumulated demand profiles for space heating and cooling. A substantial amount of heating and cooling demands can be balanced in this district, which is indicated by a demand overlap coefficient (DOC) of 0.30 [40].

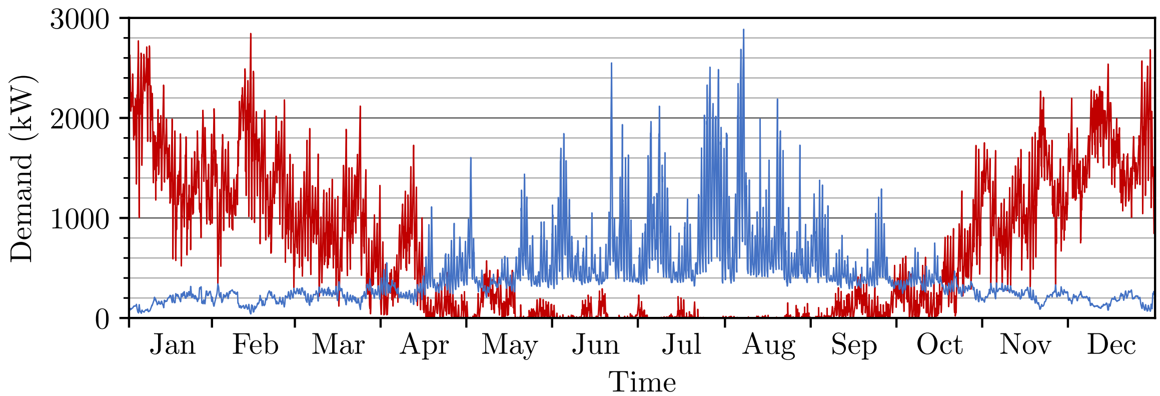

Figure 5: Cumulated space heating (red) and cooling (blue) demands of all buildings.

4. Results

In this section, the results of the case study are presented and discussed. First, the decomposition approach is validated by comparing its results with the results of the full formulation in Section 4.1. Then, the optimal energy system obtained with the decomposed models are presented in detail in Section 4.2. Finally, a parameter and sensitivity analysis on the district size (number of buildings) and the temporal resolution (number of design days) is presented in Section 4.3.

4.1. Validation of decomposition approach

In this section, the decomposition approach is validated by comparing its optimization results with the results of the full model formulation. In order to be able to obtain results from the full formulation within a reasonable computational time, a reduced district size is considered in this validation. As a result, only 4 of the 25 buildings are included and the number of design days is set to 6. For the reduced district size, the full formulation comprises 24239 continuous and 588 binary variables. In the decomposed formulation, the master problem comprises 19564 continuous decision variables and for every subproblem 1178 continuous and 147 binary variables. The solution time (excluding model setup) of the full formulation is 295 s (MIP gap: 0.1 %). In comparison, the sum of the solution times of all master and subproblems of all iterations is 50.1 s (including the final master problem with binary weights). In this study, all calculations are performed using an Intel Xeon E5-2667 CPU and Gurobi (version 9.1.1) as solver.

The objective value (total annualized costs) of the full formulation is 179 122 EUR and has a lower bound of 178 944 EUR (relaxed problem). The iteration of the last master problem with continuous weighting variables $\lambda_{i,j}$ results in an objective value of 179 066 EUR. As described in Section 2.2 and depicted in the flow chart in Fig. 3, after the last iteration the master problem is solved again with binary (instead of continuous) weighting variables $\lambda_{i,j}$ in order to ensure feasibility of the optimal solution of the decomposed formulation. The objective value of this final master problem is 179 092 EUR and lies within the MIP gap of the full formulation: It is lower than the objective value of the full formulation (179 122 EUR) but higher than the lower bound (178 944 EUR).

The results show the equivalence between the full formulation and the decomposition approach with respect to the objective function for a district with 4 buildings. The equivalence of the optimization approaches is also backed up by the results of the sensitivity analysis in Section 4.3.

4.2. Energy system optimization

In this section, the optimal energy system design for the entire district with 25 buildings is presented. This solution is obtained with the decomposed model and 12 design days. The total annualized costs of the system (objective value of the final binary master problem) is 552 746 EUR. The total solution time is 3203 s, which comprises a total of 19 s for all relaxed master problems (i.e. 3 s per solution), 7 s for the final master problem with binary weighting factors and 3177 s for all subproblems of all iterations (i.e. 21 s per subproblem).

4.2.1. Optimal system design

The optimal design of the energy hub comprises the reversible heat pump with an electric capacity of $220\,\mathrm{kW_{el}}$ (equivalent to $1040\,\mathrm{kW_{th}}$ with a nominal COP of 4.76 according to manufacturer data). The optimal capacity of the heat storage in the energy hub is 5.5 MWh. In order to generate electricity onsite, PV modules with a peak capacity of $2\,\mathrm{MW_p}$ are installed. The optimal battery capacity is 1 MWh, which is equal to the lower bound of the minimum battery capacity, c.f. Eq. (32).

As expected, most of the heat demands are covered with heat pumps. As a result, the total heat pump capacity installed in buildings is $422\,\mathrm{kW_{el}}$ (equivalent to $1996\,\mathrm{MW_{th}}$). In addition, electric heaters are installed which cover peak heat demands and offer additional operational flexibility. The total capacity of electric heaters in all buildings is $491\,\mathrm{kW_{th}}$. The total capacity of all decentral heat storages is 1.78 MWh which equals about 1/3 of the heat storage capacity in the energy hub.

4.2.2. System operation and shadow prices

In addition to the results of the optimal design, the analysis of the system operation provides further insights: In Fig. 6, the energy hub operation is depicted for a design day in winter. In the plot on the top, the heating and cooling balance for the energy hub is shown. Red areas show the heat generation by the reversible air-source heat pump. The orange and yellow areas represent heat flows charging and discharging the heat storage. The black line shows the thermal demand of all buildings that needs to be covered by the energy hub. In the middle plot, the electric power flows are illustrated: Yellow areas show PV generation, light gray areas electricity import from the grid and dark gray areas electric power from the battery. The black line represents the electricity demand of the BESs (heat pumps and electric heaters) and the green line the electricity demand of the central air-source heat pump. The plot on the bottom shows the shadow prices for electricity and heat derived from the master problem. On the depicted winter day, the 5GDHC network has a residual heat demand of about 1 MW, which is mainly covered by the air-source heat pump. In times with high electricity prices, for example in the morning hours and evening hours, the heat storage is discharged to reduce the heat pump's operation. During times with lower electricity prices, for example during the afternoon hours, the heat storage is charged using the air-source heat pump. Other effects which foster the operation of the air-source heat pump during the afternoon are the higher COPs (which result from the higher ambient air temperature during the afternoon) and the high PV generation.

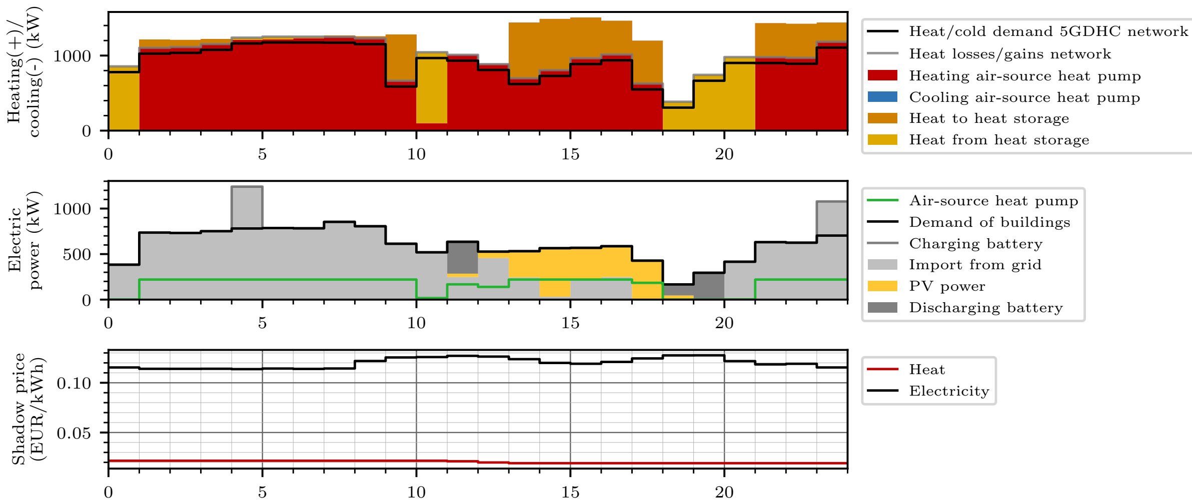

Figure 6: Energy hub operation on a winter day with high heat demands. The heat storage is charged during the afternoon using PV power, low electricity prices and higher COPs. During the morning and evening hours, when electricity prices are high, the heat storage is discharged.

An exemplary summer day is illustrated in Fig. 7. Throughout the day, the 5GDHC network has a residual cooling load. The load is covered by the air-source heat pump (in cooling mode) and the heat storage. During the afternoon, surplus heat from the network is stored in the heat storage. In the evening and night hours, the heat storage is cooled down using the heat pump. An excess of PV generation occurs during the afternoon hours. This leads to a drop of the electricity price to the level of the feed-in tariff. Due to the residual cooling load, the shadow prices for heat are negative. For the BESs (subproblems), this means a negative price for heat or, equivalently, a positive price for cooling energy.

The results of the case study show that a reasonable technology sizing is obtained using the decomposition approach.

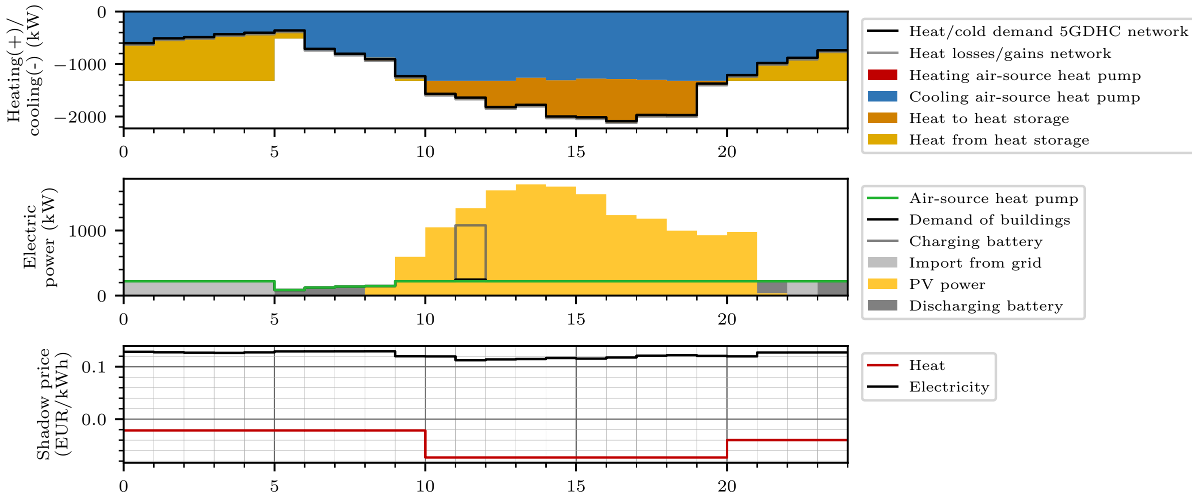

Figure 7: Operation of the energy hub during a hot summer day with residual cooling load from the 5GDHC network. The air-source heat pump cools the network and runs throughout the day. Peak cooling loads are covered with the central heat storage.

4.2.3. Analysis of shadow prices

The shadow price signals for heat (red) and electricity (green) are depicted in Fig. 8 for the design year. In addition, the residual load of the 5GDHC network (after demand balancing in the network) is depicted in gray. The illustration helps to analyze how heat prices derived from the optimization and the load situation in the 5GDHC network are related to each other. For hours with residual heating demand in the network, the heat price is positive. In contrast, if cooling demands exceed heating demands, the heat price becomes negative. The heat price ranges between −7.3 EUR-ct/kWh and +6.0 EUR-ct/kWh. The electricity price is mainly driven by the import price for electricity from the grid. It ranges between 6.5 EUR-ct/kWh and +14.1 EUR-ct/kWh with an average of 11.9 EUR-ct/kWh. The maximum heat prices occur on days with high residual heating demands in winter. Similarly, the highest negative prices (peak cooling prices) result from a design day with a high cooling load in summer.

4.3. Runtime and scalability

The main advantage of the decomposition approach is that the computational time for large districts is substantially lower compared to the full formulation. With a spatial decom-

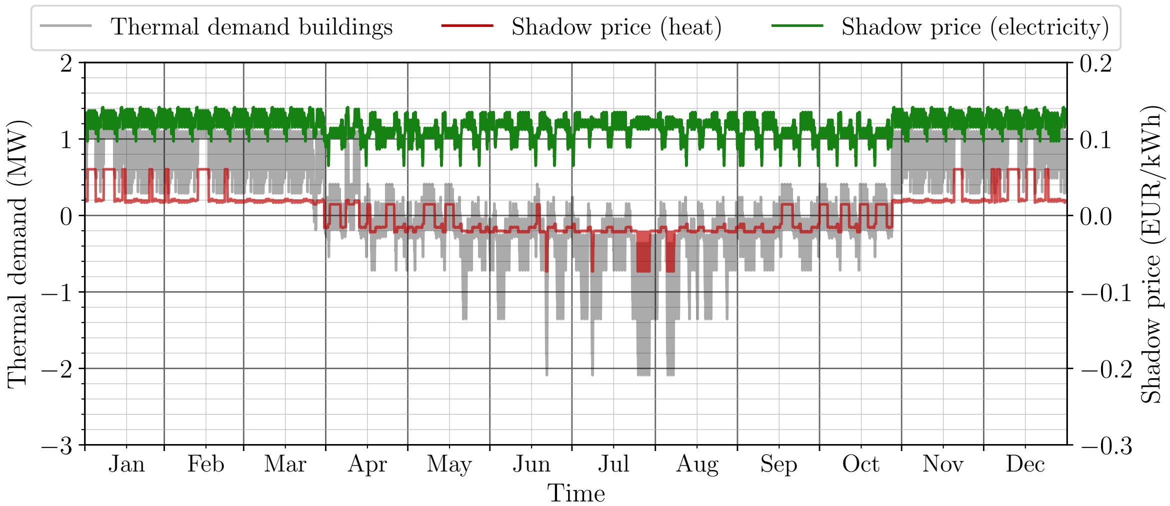

Figure 8: Shadow prices for heat and electricity as well as the residual thermal load of the 5GDHC network. A positive load means a residual heat demand, a negative load means a surplus of waste heat (cooling demand).

position, for every additional building, one additional subproblem has to be solved in each iteration. Therefore, the computational time is expected to increase approximately linearly with the number of buildings. The scalability of the decomposition approach is investigated in this section in further detail. For the solution of the full model formulations, a MIP gap of 0.1 % was used.

4.3.1. Spatial scalability: Number of buildings

A sensitivity analysis is conducted in which the number of buildings is varied. If the number of buildings exceeds 25 (the number of buildings in the use case), buildings are duplicated in order to create districts with more than 25 buildings. In this analysis, 6 design days are used in the model and a time limit is introduced in order to terminate the full formulation if the solution exceeds 1 hour. In Fig. 9, the solution time of the decomposition approach is depicted for districts with up to 100 buildings. As a comparison, the solution times of the full formulation are depicted in blue. For a district with only 2 buildings, the solution time of the decomposition approach is 18 s and the solution time for the district with 100 buildings is 1126 s. The solution times of the full formulation increase progressively: The solution of the full formulation with 2 buildings is 14 s and with 8 buildings the solution time is 642 s. For districts with more than 20 buildings, the solution time exceeds the time limit of 1 hour. The progressive increase of the solution time is expected since typically, the time to solve an MILP increases non-linearly with increasing number of variables and constraints. In contrast, the computational time of the decomposition approach increases approximately linearly with the number of buildings because for every building in the district, one subproblem is solved in each iteration and the individual solution time of the subproblems does not depend on the total number of buildings in the district.

In summary, the results show that for districts with a small number of buildings, the differences in the computational times between both optimization approaches are small. However, with increasing number of buildings, the computational times of the full formulation rapidly increase. This can be successfully tackled with the presented decomposition approach.

4.3.2. Temporal scalability: Number of design days

In addition to the spatial scalability, the sensitivity of the solution times regarding the temporal resolution is analyzed. In Fig. 10, the solution times for different numbers of design days are depicted. Here again, a district with a reduced number of 6 buildings is investigated in order to obtain results for the full formulation within a reasonable time. The solution time of the decomposition approach (red) increases approximately linearly: For less than 8 design days, the solution time is below 100 s, for 24 design days it increases to 358 s. The solution times of the full formulation increase progressively with increasing number of design days: For problems with 10 or more design days, no solution can be obtained within the time limit of 1 hour.

The equivalence of the optimization approaches is confirmed by an analysis of the objective values: The objective values for the scenarios, for which a solution of the full formulation could be obtained within the time limit (up to 8 design days), are listed in Table 2. The relative deviation between the optimization approaches is in all cases less than 0.07 %. Overall, the sensitivity analysis confirms that when the model complexity increases, the full formulation quickly becomes computationally intractable, while the decomposition model can still be solved in a reasonable amount of time.

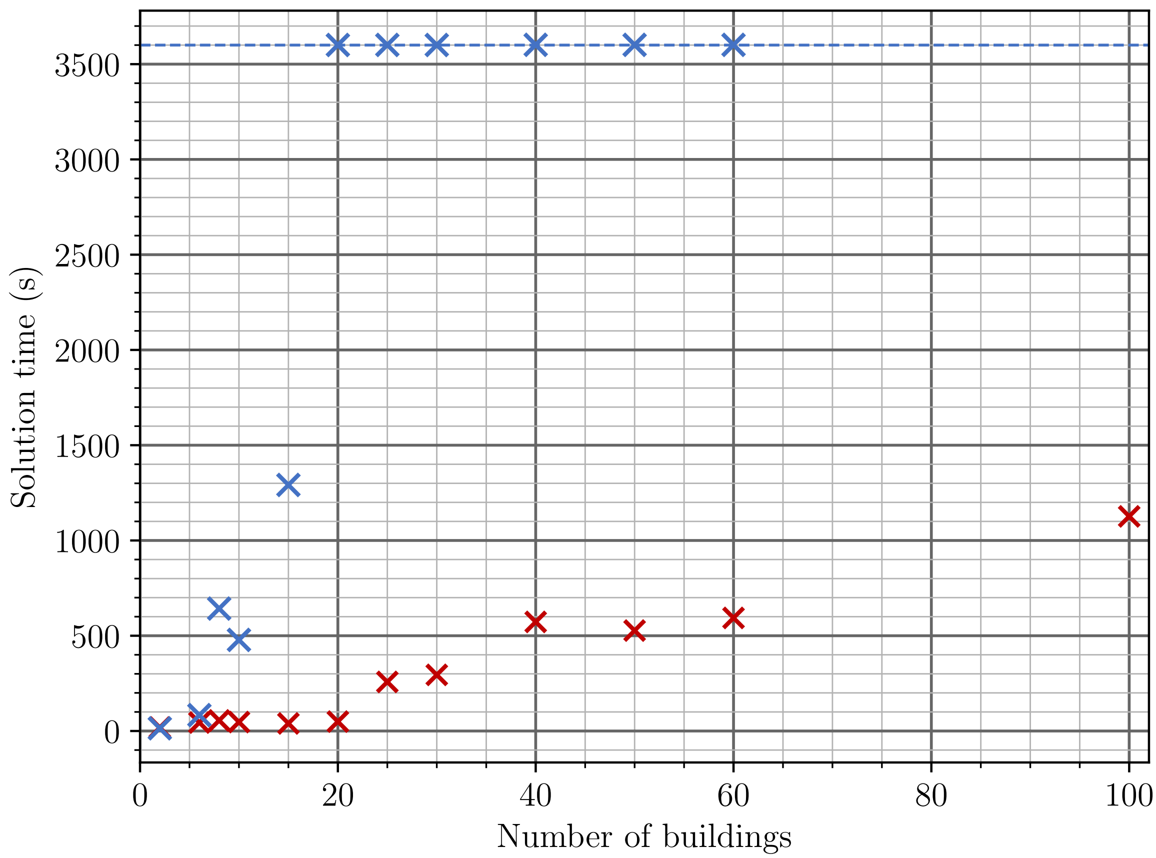

Figure 9: Solution time of the decomposition approach (red) including all subproblems and master problems as well as the solution time of the full formulation (blue) using 6 design days. The blue dashed line indicates the time limit of 1 hour.

Table 2: Objective values of the full formulation and the decomposition approach for a different number of design days.

Design days	Full formulation (EUR/a)	Decomposition approach (EUR/a)	Deviation
2	255941	255751	0.07 %
4	284538	284546	$<$ 0.01 %
6	286001	285811	0.07 %
8	278044	277978	0.02 %

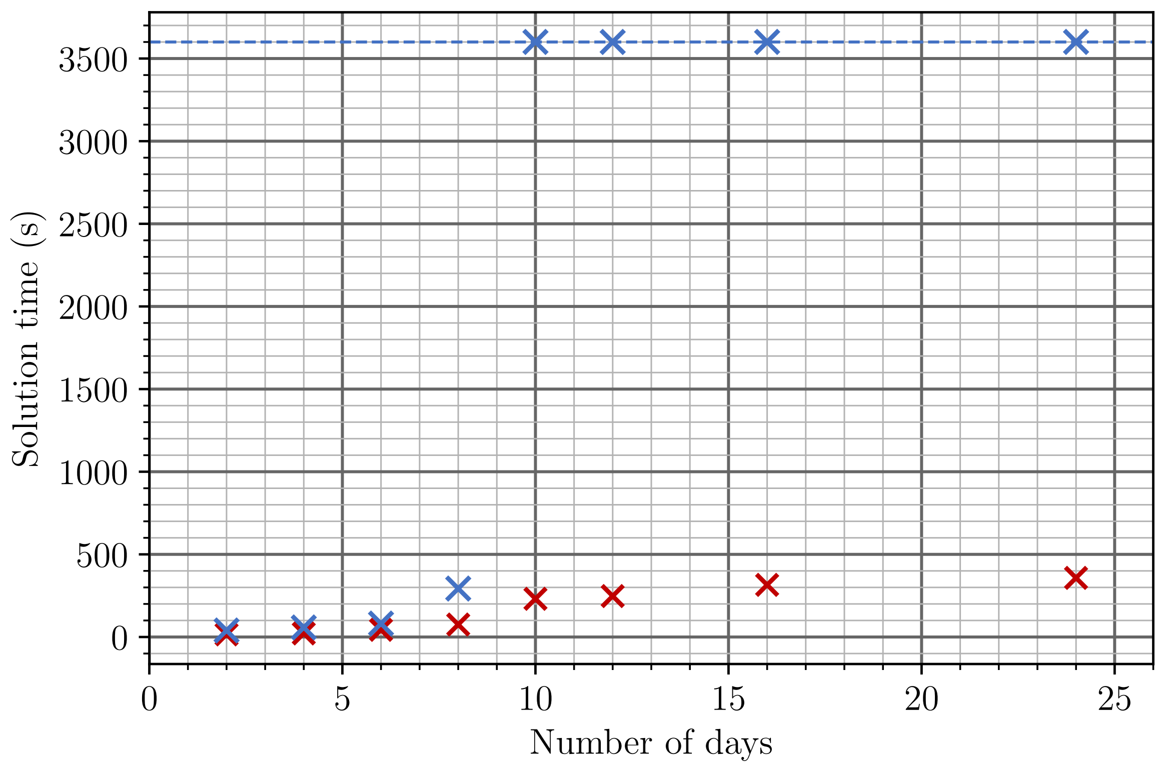

Figure 10: Solution times for the decomposed models (red) and the full formulation (blue) for a district with 6 buildings. The time limit of 1 hour for the solution of the full formulation is indicated by the blue dashed line.

5. Conclusions and outlook

5.1. Conclusions

In this paper, a decomposition approach for a design optimization model for a case study with a 5GDHC network is presented that uses a Dantzig-Wolfe decomposition and a column generation approach. For this purpose, the full model formulation is subdivided into a master problem (energy hub, microgrid and 5GDHC network) and multiple subproblems (BESs). In a first step, the equivalence of the original (full) formulation and the decomposed formulation is validated for a case study. In addition within a sensitivity analysis, it is shown that the solution time of the decomposed problem formulations increases approximately linearly with increasing number of buildings and design days. This is a central advantage over the full formulation which shows a progressive increase of its solution time. Thus, it is shown that the proposed decomposition method is suitable to solve complex 5GDHC problems more efficiently with comparable result accuracy.

In addition, the decomposition approach allows to obtain shadow prices for heat and electricity with an hourly resolution. Shadow prices represent the availability of heat and electricity in the district. Due to prosumer buildings, which feed heat or electricity into the respective network, heat and electricity prices can become negative. When there is a surplus of heat in the district (i.e. the 5GDHC network has a net cooling demand), the heat price becomes negative and buildings tend to feed in less heat into the network. The analysis of the shadow prices for heat and electricity helps to find appropriate pricing models for 5GDHC networks. In summary, the application of decomposition approaches shows a great potential to reduce computational times of MILP formulations for 5GDHC systems. Reducing computational times is especially important for the concept phase of district projects, which is characterized by a large number of planning iterations and therefore requires fast solving design models.

5.2. Outlook

In future works, the presented decomposition approach should be applied to different case studies, e. g. with a different set of technologies in the energy hub, to confirm the applicability of the method and in addition, the Dantzig-Wolfe method can be compared to other decomposition methods. Furthermore, the presented decomposition can be applied to operational optimization models, as presented in [20, 21, 22]. The authors of these studies experienced in their work high computational times already for districts with a small number of buildings.

In particular, the concept of shadow prices seems promising for complex operational optimization of 5GDHC systems: The price profiles for heat and electricity can help to derive heuristic or rule-based controls for the operation of the technologies in the buildings. Alternatively, the price signals can be used as input data for a control algorithm based on machine learning. Here, a central control can reward heat feed-in during times with net heating demands or punish the feed-in during times with net cooling demands.

6. Acknowledgments

We gratefully acknowledge the financial support by the Federal Ministry for Economic Affairs and Climate Action (BMWK), promotional reference 03EWR020E (*Reallabor der Energiewende: TransUrban.NRW*). In addition, we gratefully acknowledge the financial support by RWTH Aachen University granting a *RWTH Research Ambassador Scholarship* for the research stay of Marco Wirtz at Lawrence Berkeley National Laboratory.

7. Nomenclature

Abbreviations

5GDHC	5th generation district heating and cooling
ACC	Accumulator tank
ASHP	Air-source heat pump
BAT	Battery
BES	Building energy system
COP	Coefficient of performance
DHC	District heating and cooling
DOC	Demand overlap coefficient
DRC	Direct cooling
EB	Electric boiler
EH	Energy hub
HP	Heat pump
MILP	Mixed-integer linear program
MIQCP	Mixed-integer quadratically constrained program
PV	Photovoltaics
TES	Thermal energy storage

Indices and Sets

$b \in \mathcal{B}$	Buildings
$d \in \mathcal{D}$	Design day
$y \in Y$	Day of year
$t \in \mathcal{T}$	Time step
$k \in K$	Technology

Variables

C	Costs
cap	Generation/storage capacity
P	Electric power
Q	Thermal power
R	Revenue
S	State of charge
u	Operation decision (binary)
x	Investment decision (binary)
λ	Weighting factors

Parameters

Δt	Length of time step
η	Efficiency
a	Annuity factor
$\hat{\mathrm{M}}$	Big-M value
η	Efficiency
f	Operation & maintenance factor
c	Costs
p	Energy supply price
PLR	Minimum part-load threshold
r	feed-in tariff
w	Design day weight
ϕ	Storage loss factor
π	Shadow price (heat/electricity)
σ	Shadow price (costs)

Sub- and superscripts

c	cooling
cap	capacity
ch/dch	charge/discharge
dem	demand
el	electricity
feed-in	electricity feed-in
fix	fix investment costs
grid	electricity grid
h	heating
heat	heat
inv	investment
loss	thermal loss
max	maximum
min	minimum
nom	nominal
om	operation & maintenance
res	residual
tot	total

References

[1] European Comission, An EU Strategy on Heating and Cooling (2016).

[2] H. Lund, B. Möller, B. V. Mathiesen, A. Dyrelund, The role of district heating in future renewable energy systems, Energy 35 (3) (2010) 1381–1390. doi:10.1016/j.energy.2009.11.023.

[3] H. Lund, S. Werner, R. Wiltshire, S. Svendsen, J. E. Thorsen, F. Hvelplund, B. V. Mathiesen, 4th Generation District Heating (4GDH) Integrating smart thermal grids into future sustainable energy systems, Energy 68 (2014) 1–11. doi:10.1016/j.energy.2014.02.089.

[4] H. Lund, N. Duic, P. A. Østergaard, B. V. Mathiesen, Future district heating systems and technologies: On the role of smart energy systems and 4th generation district heating, Energy 165 (2018) 614–619. doi:10.1016/j.energy.2018.09.115.

[5] H. Lund, P. A. Østergaard, M. Chang, S. Werner, S. Svendsen, P. Sorknæs, J. E. Thorsen, F. Hvelplund, B. O. G. Mortensen, B. V. Mathiesen, C. Bojesen, N. Duic, X. Zhang, B. Möller, The status of 4th generation district heating: Research and results, Energy 164 (2018) 147–159. doi:10.1016/j.energy.2018.08.206.

[6] M. Sulzer, S. Werner, S. Mennel, M. Wetter, Vocabulary for the fourth generation of district heating and cooling, Smart Energy 1 (2021) 100003. doi:10.1016/j.segy.2021.100003.

[7] H. Lund, P. A. Østergaard, T. B. Nielsen, S. Werner, J. E. Thorsen, O. Gudmundsson, A. Arabkoohsar, B. V. Mathiesen, Perspectives on fourth and fifth generation district heating, Energy 227 (2021) 120520. doi:10.1016/j.energy.2021.120520.

[8] F. Bünning, M. Wetter, M. Fuchs, D. Müller, Bidirectional low temperature district energy systems with agent-based control: Performance comparison and operation optimization, Applied Energy 209 (2018) 502–515. doi:10.1016/j.apenergy.2017.10.072.

[9] Ruesch F., Rommel M., Scherer J., Pumping power prediction in low temperature district heating networks. Proceedings of International Conference CISBAT 2015, LESO-PB, EPFL, Lausanne. (2015) 753–758.

[10] A. Prasanna, V. Dorer, N. Vetterli, Optimisation of a district energy system with a low temperature network, Energy 137 (2017) 632–648. doi:10.1016/j.energy.2017.03.137.

[11] N. Vetterli, M. Sulzer, Dynamic analysis of the low-temperature district network Suurstoffi through monitoring: Proceedings of International Conference CISBAT 2015, LESO-PB, EPFL, Lausanne (2015) 517–522.

[12] M. Pellegrini, A. Bianchini, The Innovative Concept of Cold District Heating Networks: A Literature Review, Energies 11 (1) (2018) 236. doi:10.3390/en11010236.

[13] Stübler A., Bestenlehner D, Drück H., Energy saving potentials of cold district heating networks: Proceedings of the 17th EWA symposium during IFAT 2014, Munich. (2014).

[14] U. Eicker, Urban energy systems for low-carbon cities, Academic Press an imprint of Elsevier, London, 2019.
URL https://www.sciencedirect.com/science/book/9780128115534

[15] P. Kräuchi, M. Kolb, T. Gautschi, U.-P. Menti, M. Sulzer, Modellbildung für thermische Arealvernetzung mit IDA-ICE (2014).

[16] M. Sulzer, Kalte Fernwärme (Anergienetze). Grundlagen/Thesenpapier, Hochschule Luzern (2014).

[17] K. Filonenko, K. Arendt, M. Jradi, S. Andersen, C. Veje, Modeling and Simulation of a Heating Mini-Grid for a Block of Buildings, in: V. Corrado, E. Fabrizio, A. Gasparella, F. Patuzzi (Eds.), Proceedings of Building Simulation 2019: 16th Conference of IBPSA, Building Simulation Conference proceedings, IBPSA, 2020, pp. 1971–1978. doi:10.26868/25222708.2019.210870.

[18] M. Wirtz, L. Kivilip, P. Remmen, D. Müller, 5th Generation District Heating: A novel design approach based on mathematical optimization, Applied Energy 260 (2020) 114158. doi:10.1016/j.apenergy.2019.114158.

[19] D. Hering, A. Xhonneux, D. Müller, Design optimization of a heating network with multiple heat pumps using mixed integer quadratically constrained programming, Energy 226 (2021) 120384. doi:10.1016/j.energy.2021.120384.

[20] P. Gabrielli, A. Acquilino, S. Siri, S. Bracco, G. Sansavini, M. Mazzotti, Optimization of low-carbon multi-energy systems with seasonal geothermal energy storage: The Anergy Grid of ETH Zurich, Energy Conversion and Management: X (2020) 100052doi:10.1016/j.ecmx.2020.100052.

[21] M. Wirtz, L. Neumaier, P. Remmen, D. Müller, Temperature control in 5th generation district heating and cooling networks: An MILP-based operation optimization, Applied Energy 288 (2021) 116608. doi:10.1016/j.apenergy.2021.116608.

[22] D. Hering, M. E. Cansev, E. Tamassia, A. Xhonneux, D. Müller, Temperature control of a low-temperature district heating network with Model Predictive Control and Mixed-Integer Quadratically Constrained Programming, Energy 224 (2021) 120140. doi:10.1016/j.energy.2021.120140.

[23] M. Wirtz, M. Hahn, T. Schreiber, D. Müller, Design optimization of multi-energy systems using mixed-integer linear programming: Which model complexity and level of detail is sufficient?, Energy Conversion and Management 240 (2021) 114249. doi:10.1016/j.enconman.2021.114249.

[24] George B. Dantzig, Philip Wolfe, Decomposition Principle for Linear Programs, Operations Research 8 (1) (1960) 101–111.
URL http://www.jstor.org/stable/167547

[25] R. Yokoyama, Y. Hasegawa, K. Ito, A MILP decomposition approach to large scale optimization in structural design of energy supply systems, Energy Conversion and Management 43 (6) (2002) 771–790. doi:10.1016/S0196-8904(01)00075-9.

[26] H. Harb, J.-N. Paprott, P. Matthes, T. Schütz, R. Streblow, D. Müller, Decentralized scheduling strategy of heating systems for balancing the residual load, Building and Environment 86 (2015) 132–140. doi:10.1016/j.buildenv.2014.12.015.

[27] G. Belov, G. Scheithauer, A branch-and-cut-and-price algorithm for one-dimensional stock cutting and two-dimensional two-stage cutting, European Journal of Operational Research 171 (1) (2006) 85–106. doi:10.1016/j.ejor.2004.08.036.

[28] T. Schütz, X. Hu, M. Fuchs, D. Müller, Optimal design of decentralized energy conversion systems for smart microgrids using decomposition methods, Energy 156 (2018) 250–263. doi:10.1016/j.energy.2018.05.050.

[29] T. Wakui, M. Hashiguchi, R. Yokoyama, Structural design of distributed energy networks by a hierarchical combination of variable- and constraint-based decomposition methods, Energy 224 (2021) 120099. doi:10.1016/j.energy.2021.120099.

[30] T. Wakui, M. Hashiguchi, R. Yokoyama, A near-optimal solution method for coordinated operation planning problem of power- and heat-interchange networks using column generation-based decomposition, Energy 197 (2020) 117118. doi:10.1016/j.energy.2020.117118.

[31] VDI 2067-1. Economic efficiency of building installations - Fundamentals and economic calculation. Technical report., Beuth Verlag GmbH (2012).

[32] P. Gabrielli, M. Gazzani, E. Martelli, M. Mazzotti, Optimal design of multi-energy systems with seasonal storage, Applied Energy 219 (2018) 408–424. doi:10.1016/j.apenergy.2017.07.142.

[33] T. Zamfirescu, Minkowski's theorem for arbitrary convex sets, European Journal of Combinatorics 29 (8) (2008) 1956–1958. doi:10.1016/j.ejc.2008.01.021.

[34] H. Harb, J.-N. Paprott, P. Matthes, T. Schütz, R. Streblow, D. Müller, Decentralized scheduling strategy of heating systems for balancing the residual load, Building and Environment 86 (2015) 132–140. doi:10.1016/j.buildenv.2014.12.015.

[35] Deutsche Norm, DIN EN 13941: Auslegung und Installation von gedämmten Einzel- und Doppelrohr-Verbundsystemen für direkt erdverlegte Heißwasser-Fernwärmenetze (2019).

[36] F. Domínguez-Muñoz, J. M. Cejudo-López, A. Carrillo-Andrés, M. Gallardo-Salazar, Selection of typical demand days for CHP optimization, Energy and Buildings 43 (11) (2011) 3036–3043. doi:10.1016/j.enbuild.2011.07.024.

[37] T. Schütz, M. H. Schraven, M. Fuchs, P. Remmen, D. Müller, Comparison of clustering algorithms for the selection of typical demand days for energy system synthesis, Renewable Energy 129 (2018) 570–582. doi:10.1016/j.renene.2018.06.028.

[38] P. Remmen, M. Lauster, M. Mans, M. Fuchs, T. Osterhage, D. Müller, TEASER: an open tool for urban energy modelling of building stocks, Journal of Building Performance Simulation 11 (1) (2017) 84–98. doi:10.1080/19401493.2017.1283539.

[39] U. Jordan, K. Vajen, Dhwcalc: Program to generate domestic hot water profiles with statistical means for user defined conditions (2005).

[40] M. Wirtz, L. Kivilip, P. Remmen, D. Müller, Quantifying Demand Balancing in Bidirectional Low Temperature Networks, Energy and Buildings 224 (2020) 110245. doi:10.1016/j.enbuild.2020.110245.